

TLR9 protects non-immune cells from stress by modulating mitochondrial ATP synthesis through the inhibition of SERCA2

Yasunori Shintani^{1,4}, Hannes CA Drexler², Hidetaka Kioka³, Cesare MN Terracciano⁶, Steven R Coppen¹, Hiromi Imamura⁷, Masaharu Akao⁸, Junichi Nakai⁹, Ann P Wheeler¹⁰, Shuichiro Higo³, Hiroyuki Nakayama⁵, Seiji Takashima^{3,4}, Kenta Yashiro¹ and Ken Suzuki¹

¹ William Harvey Research Institute, Barts and The London School of Medicine and Dentistry, Queen Mary University of London, Charterhouse Square, London EC1M 6BQ, UK

² Bioanalytical Mass Spectrometry, Max Planck Institute for Molecular Biomedicine, Röntgenstr. 20, 48149 Muenster, Germany

³ Department of Cardiovascular Medicine, ⁴ Department of Medical Biochemistry, Osaka University Graduate School of Medicine, Suita, Osaka 565-0871, Japan

⁵ Laboratory of Clinical Science and Biomedicine, Osaka University Graduate School of Pharmaceutical Sciences, Osaka 565-0871, Japan

⁶ Laboratory of Myocardial Electrophysiology, Imperial Centre for Translational and Experimental Medicine, Imperial College London, National Heart & Lung Institute, Hammersmith Campus, Du Cane Road, London W12 0NN, UK

⁷ The Hakubi Center & Graduate School of Biostudies, Kyoto University Science Frontier Laboratory building Room 305, Faculty of Medicine Campus, Kyoto 606-8501, Japan

⁸ Department of Cardiology, National Hospital Organization Kyoto Medical Center, Kyoto 612-8555, Japan

⁹ Saitama University Brain Science Institute, Saitama City 338-8570, Japan

¹⁰ Blizard Advanced Light Microscopy Facility, Blizard Institute, Barts and The London School of Medicine and Dentistry, Queen Mary University of London, London E1 2AT, UK

Correspondence,

Yasunori Shintani or Ken Suzuki

yshintani@medbio.med.osaka-u.ac.jp or ken.suzuki@qmul.ac.uk

Tel +44 2078828236 FAX +44 2078828256

Abstract

Toll-like receptor 9 (TLR9) has a key role in the recognition of pathogen DNA in the context of infection and cellular DNA that is released from damaged cells. Pro-inflammatory TLR9 signalling pathways in immune cells have been well investigated, but we have recently discovered an alternative pathway in which TLR9 temporarily reduces energy substrates to induce cellular protection from stress in cardiomyocytes and neurons. However, the mechanism by which TLR9 stimulation reduces energy substrates remained unknown. Here, we identify the calcium-transporting ATPase, SERCA2 (also known as Atp2a2), as a key molecule for the alternative TLR9 signalling pathway. TLR9 stimulation reduces SERCA2 activity, modulating Ca^{2+} handling between the SR/ER and mitochondria, which leads to decrease in mitochondrial ATP levels and the activation of cellular protective machinery. These findings reveal how distinct innate responses can be elicited in immune and non-immune cells—including cardiomyocytes—using the same ligand-receptor system.

INTRODUCTION

Extracellular DNA released from damaged tissue is a sign of danger. In the danger model [1,2], the self-molecules released from damaged cells (the damage-associated molecular patterns (DAMP)) are sensed by DAMP receptors on immune cells, triggering an inflammatory response. Toll-like receptors (TLRs) form a major group of DAMP receptors. Among TLRs, TLR9 is the only receptor for detecting DNA (self and non-self) [3], and hence the DNA released from damaged cells can trigger inflammation *via* TLR9 in immune cells [2]. Naturally, TLR9 is expressed in immune cells, however, its expression was also reported in non-immune cells including cardiomyocytes and neurons [4,5]. It would be very damaging for such organs with poor regenerative capacity, if TLR9 in non-immune cells also operates the inflammatory signalling that increases tissue damage.

Recently we have reported an alternative function of TLR9 to induce cellular protection in cardiomyocytes and neurons [6]. We found that CpG-oligodeoxynucleotide (CpG-ODN; TLR9 ligand) temporally reduces energy substrates to protect cardiomyocytes and neurons by activating AMP-activated protein kinase (AMPK) without inducing canonical inflammatory signalling. Comparison of the expression profiles between cardiomyocytes and macrophages and subsequent functional studies identified that the expression level of *Unc93b1* is a pivotal switch for the distinct TLR9 responses by regulating subcellular localization of TLR9. *Unc93b1* is a chaperon-like protein that helps TLR9 travel from the ER to endosome to become the N-terminally shed, immune-prone type of receptor. After ligand stimulation, this cleaved TLR9 subsequently forms a signalling molecular complex with MyD88 to initiate inflammatory signalling in macrophages [7,8]. On the contrary, under low expression of *Unc93b1* in non-immune cells including cardiomyocytes and differentiated neurons, endocytosed DNA is transported to the ER *via* the retrograde route to bind the TLR9 that stays at the ER, subsequently decreases energy substrates and increases the AMP/ATP ratio, then activates AMPK [6]. However, the molecular mechanism by which TLR9 in the ER reduces intracellular ATP levels remains unknown.

RESULTS AND DISCUSSION

SERCA2 is an adaptor for the alternative TLR9 signalling

The known inflammatory TLR9 signalling is mediated by a common TLR adaptor molecule, MyD88 [9]. However, we have recently demonstrated that the modulation of energy metabolism through TLR9 still operates in MyD88^{-/-} cardiomyocytes [6], suggesting that this alternative TLR9 signalling is MyD88-independent and branches from the pro-inflammatory TLR9 signalling at the receptor level.

To identify adaptor molecules for the alternative, cellular protective TLR9 signalling, tandem affinity purification was performed in primary rat neonatal cardiomyocytes (alternative TLR9 signal; on) and cardiac fibroblasts for comparison (alternative TLR9 signal; off) using adenoviral vectors that encoded full-length TLR9 tagged with a HA-FLAG at the C-terminus (TLR9-HA-FLAG) or YFP-HA-FLAG. The comparison of TLR9 immunoprecipitates revealed the existence of a 95-kDa band associated with TLR9 in cardiomyocytes, but not in cardiac fibroblasts (Fig 1A). Importantly, intensity of this 95-kDa band was increased after CpG-ODN stimulation (Fig 1B). Mass spectrometric analysis identified this protein as sarcoplasmic reticulum (SR) Ca²⁺ ATPase, SERCA2.

The association between TLR9 and SERCA2 was verified by a series of observations. First, reciprocal co-immunoprecipitation by SERCA2 demonstrated its binding to the overexpressed TLR9 in cardiomyocytes (Supplementary Fig S1A online).

Second, to exclude the possibility that the SERCA2 and TLR9 association might be an artifact due to the TLR9 overexpression, we checked for endogenous association between TLR9 and SERCA2 using mouse neonatal cardiomyocytes treated with a cell-permeable crosslinker, dithiobis[succinimidylpropionate] (DSP) [10]. As shown in Fig 2A, TLR9 that was co-immunoprecipitated with SERCA2 was clearly detected in wild-type cardiomyocytes, but not in TLR9^{-/-} cardiomyocytes, confirming the association was unrelated to the overexpression of TLR9.

Third, to further confirm its specific binding, we added non-biased proteomics analysis of TLR9 immunoprecipitates from rat neonatal cardiomyocytes and cardiac fibroblasts. Most of heat shock proteins and ribosomal proteins were found in the immunoprecipitates from both cell types, which are major non-specific binding proteins from immunoprecipitates with an overexpressed bait (Supplementary Fig S1B online) [11]. In this approach, we again confirmed SERCA2 to be a cardiomyocyte-specific TLR9 binding protein, while other abundant Ca²⁺ pump proteins in cardiomyocytes, such as ryanodine receptor (RyR) or inositol 1,4,5-triphosphate receptor (IP₃R), were not detected in the immunoprecipitates from cardiomyocytes (Supplementary Fig S1B online). These data also support our finding that SERCA2 is a TLR9 associating protein.

Finally, immunofluorescence studies demonstrated that not only the overexpressed TLR9-HA-FLAG protein colocalized with SERCA2 and with the ER/SR marker KDEL in cardiomyocytes (Fig 2B and Supplementary Fig S1C online), but also the endogenous TLR9 colocalized with SERCA2 (Fig 2C). Collectively from these data, we conclude that TLR9 interacts with SERCA2 at ER/SR in cardiomyocytes.

TLR9 reduces SERCA2 activity and Ca²⁺ content in the ER/SR in cardiomyocytes

To confirm the functional involvement of SERCA2 in the alternative TLR9 signalling, we performed a knockdown experiment of *SERCA2* in cardiomyocytes. Different siRNAs targeting *SERCA2* efficiently abolished the CpG-induced activation of AMPK (Fig 3A), suggesting that SERCA2 indeed plays a pivotal role in the alternative TLR9 signalling in cardiomyocytes.

SERCA2 is an ER/SR-resident Ca²⁺-ATPase that governs Ca²⁺ uptake from the cytosol to ER/SR and regulates Ca²⁺ storage in the ER/SR. Given that SERCA2 has an enzymatic activity and that the binding between TLR9 and SERCA2 was enhanced by ligand stimulation (Fig 1B), we hypothesized if TLR9 stimulation could modulate SERCA2 activity. First, by measuring Ca²⁺-ATPase activity of SERCA2 in neonatal cardiomyocytes with or without CpG-ODN treatment, we found that TLR9 stimulation, indeed, significantly reduced SERCA2 activity (Fig 3B). Next, to directly monitor Ca²⁺ in the SR/ER in living cardiomyocytes, we used a SR/ER-targeting Förster resonance energy transfer (FRET)-based Ca²⁺ indicator, D1ER [12], by adenovirus-mediated delivery. Time-lapse observation demonstrated that CpG-ODN significantly reduced Ca²⁺ in the SR/ER from 10 min after administration (Fig 3C and D). As Ca²⁺ storage (Ca²⁺ content) in the ER/SR controls the time course of the cytosolic Ca²⁺ concentration during each cardiac beating cycle (Ca²⁺ transient), next we analysed Ca²⁺ content and Ca²⁺ transient with or without CpG-ODN treatment using rat adult cardiomyocytes. SR Ca²⁺ content measured by caffeine-induced amplitude of Ca²⁺ transient (caffeine-induced F/F₀) was significantly reduced at 30 min after CpG administration (Fig 3E). As a consequence, the administration of CpG-ODN reduced the amplitude of Ca²⁺ transient (F/F₀), Ca²⁺ decay (mostly dependent on ER/SR Ca²⁺ re-uptake) and time to peak (an indication of speed of ER/SR Ca²⁺ release) in the Ca²⁺ transient (Fig 3F and G). All these results indicate that SERCA2 activity is reduced by TLR9 stimulation.

Next, we tested if SERCA2 inhibition is sufficient to switch on the alternative TLR9 signalling. To this end, we exploited the property of a low molecular weight compound, thapsigargin as a SERCA2 inhibitor. We observed that short periods of thapsigargin treatment alone effectively increased AMPK phosphorylation in cardiomyocytes (Fig 3H), suggesting that modulation of Ca²⁺ handling is sufficient to achieve the same outcome as that of the alternative TLR9 signalling. Thapsigargin is an irreversible SERCA2 inhibitor and inhibiting SERCA2 by thapsigargin for hours is known to induce ER stress [13,14]. However, as demonstrated in Fig 3I, expression levels of *GRP 78* and *94* remained unchanged at 1 or 3 hours after the administration of CpG-ODN, suggesting no substantial damage in the ER, presumably because CpG-ODN-induced decrease in SERCA2 activity was incomplete, transient and reversible [6].

From these results, we conclude that SERCA2 is a functioning adaptor that mediates the alternative TLR9 signalling in cardiomyocytes.

TLR9 reduces mitochondrial ATP synthesis by alteration of ER/mitochondria Ca²⁺ handling *via* SERCA2

The next question is how TLR9 reduces the ATP levels by decreasing SERCA2 activity. Not only

several mitochondrial matrix dehydrogenases in the TCA cycle, but also almost all steps in oxidative phosphorylation (OXPHOS) are positively regulated by the level of mitochondrial Ca^{2+} ($[\text{Ca}^{2+}]_m$) [15], and close proximity between ER/SR and mitochondria is a key for the regulation of $[\text{Ca}^{2+}]_m$ [16]. Immediately after Ca^{2+} release from the ER/SR, local Ca^{2+} concentration in the space between ER/SR and mitochondria will be high enough for the mitochondrial calcium uniporter to be activated. Therefore Ca^{2+} handling between the ER/SR and mitochondria plays a critical role in the regulation of mitochondrial ATP synthesis [17,18]. Hence, we examined whether TLR9 modulates Ca^{2+} handling between these organelles in cardiomyocytes. First, using a mitochondria-targeting Ca^{2+} probe, G-CaMP2-*mt* [19], we found that $[\text{Ca}^{2+}]_m$ significantly dropped following the CpG-ODN administration (Fig 4A and B). In addition, thapsigargin administration without CpG-ODN effectively decreased $[\text{Ca}^{2+}]_m$ in cardiomyocytes (Supplementary Fig S2A online), suggesting that modulation of $[\text{Ca}^{2+}]_m$ in the alternative TLR9 signalling was mediated by SERCA2 inhibition.

Next, to further confirm a link between the decreased $[\text{Ca}^{2+}]_m$ and mitochondrial ATP synthesis, we measured mitochondrial ATP levels at the single cell level using a mitochondria-targeting FRET-based ATP probe, mit-ATeam [20,21]. Adenovirus-mediated delivery of mit-ATeam enabled us to monitor the mitochondrial ATP levels (Fig 4C). Using this biosensor, we found that administration of CpG-ODN reduced the mitochondrial ATP levels in cardiomyocytes (Fig 4D), indicating that TLR9 can indeed decrease mitochondrial ATP synthesis. Collectively from these data, we concluded that TLR9 signalling in cardiomyocytes modulates energy metabolism by altering $[\text{Ca}^{2+}]_m$ *via* decreased SERCA2 activity, leading to decrease in mitochondrial ATP synthesis, which subsequently switches on AMPK, whose activation leads to increased stress tolerance [6].

The main finding of this study is that SERCA2 is a key functioning adaptor/mediator for the alternative TLR9 signalling in cardiomyocytes. Our data showed that alternative TLR9 signalling decreased SERCA2 activity but did not cause detectable ER stress. As the alternative TLR9 signalling that decreases energy substrate and activates AMPK is transient [6], we speculated SERCA2 inhibition by TLR9 is relatively short, reversible and partial, while in contrast thapsigargin is an irreversible SERCA2 inhibitor and causes ER stress when its inhibition is long-term. Indeed, it has been known that a number of drugs that reversibly inhibit mitochondrial respiration improve recovery from ischemia reperfusion injury [22].

While we used synthetic TLR9 ligand (CpG-ODN) throughout this study, mitochondrial DNA, which is rich in unmethylated CpGs and is therefore a potent ligand for TLR9, also induced AMPK activation in cardiomyocytes in the same manner as synthetic CpG-ODN [6]. Given that cardiomyocytes possess abundant mitochondria, it is likely that substantial amount of mitochondrial DNA would be released extracellularly in the heart upon tissue damage.

We previously demonstrated that differentiated neuronal cells also operate the alternative TLR9 signalling [6]. Ca^{2+} uptake from the cytosol to ER is regulated by a ubiquitous/housekeeping splicing isoform of SERCA2, SERCA2b, in most cell types except for cardiomyocytes where SERCA2a is predominantly expressed [23]. By using the isoform-specific antibodies [24], we found that the both isoforms associated with TLR9 (Supplementary Fig S2B online), suggesting

TLR9-SERCA2 association can be applied to other cell types. We have shown that the expression level of *Unc93b1* is a pivotal switch for the distinct TLR9 responses between cardiomyocytes and macrophage-like cell line RAW264.7; knockdown of *Unc93b1* transformed the response to CpG-ODN in RAW264.7 cells from the inflammatory to the alternative TLR9 signalling, and vice versa [6]. Indeed, the interaction between TLR9 and SERCA2 became evident in *Unc93b1* knocked-down RAW264.7 cells, while no such interaction in control cells (Supplementary Fig S2C online). These data suggest that the stored Ca^{2+} in the ER/SR is released from RyR in myocytes or from IP_3R in other cell types upon stimulation and/or constitutive focal activation [17], and is then transferred to mitochondria through the local mitochondrial calcium uniporter. Both types of Ca^{2+} release contribute to the maintenance of average $[\text{Ca}^{2+}]_m$, and hence mitochondrial bioenergetics.

In our previous report, TLR9 in cardiomyocytes was found only in the ER, but was not transported to the endosome regardless of CpG stimulation [6]. In addition, we were not able to detect cleaved TLR9 in cardiomyocytes. Further, the retrogradely transported DNA was found in the ER in the *Unc93b1* knocked-down RAW264.7 cells, in which TLR9 cleavage was inhibited. Thus, we believe that retrograde transport of CpD-DNA does not require TLR9 cleavage and in cardiomyocytes TLR9 binds to CpG-ODN in the ER in an uncleaved form, subsequently interact with SERCA2. According to the work of Miyake's group [25], a bona-fide inflammatory TLR9 receptor complex (TLR9N + TLR9C) requires *Unc93b1* expression and TLR9 cleavage in the endosome, which is consistent with our model. We also showed that TLR7 ligand also triggers the alternative TLR9 signalling as to AMPK activation, while TLR2 and 4 ligands do not induce the same response [6]. TLR 3 and 7 also use *Unc93b1*-dependant transport system from the ER to endosome, therefore it is likely that other intracellular TLRs are capable of interacting with SERCA2 in the cells with low expression level of *Unc93b1*.

In this report, we uncovered the mechanism of the alternative TLR9 signalling in cardiomyocytes and we proposed a model that the same ligand-receptor system induces distinct biological responses upon tissue injury. (Fig 4E). Mimicking the alternative TLR9 signalling, inhibition of mitochondrial ATP synthesis, might have therapeutic potential against myocardial infarction or other sterile inflammation. Notably, as the distinct TLR9 signalling pathways are separated at the receptor level, enhancing the protective effect will work synergistically with the inhibition of unnecessary canonical inflammatory signalling, e.g. MyD88 inhibition or *Unc93b1* knockdown.

METHODS

Plasmids

Mouse TLR9-myc cDNA was a kind gift from Dr Brinkmann. C-terminal myc was replaced with HA-FLAG tag by a PCR-based method and the sequence was confirmed.

Tandem affinity purification

Cardiomyocytes or fibroblasts transfected with adenovirus expressing HA-FLAG-tagged TLR9 or YFP were lysed in lysis buffer (20 mM MOPS, pH 7.4, 10% glycerol, 0.15 M NaCl, 0.5% CHAPS, 1 mM EDTA, protease inhibitor cocktail (Sigma)) and immunoprecipitated with anti-FLAG M2 agarose (Sigma) at 4°C for 1 hr. The beads were washed and eluted with buffer containing 0.25 mg/ml 3xFLAG peptide (Sigma) at 4°C for 15 min. After removal of the FLAG-agarose, the eluates were immunoprecipitated with anti-HA matrix (Roche, clone 12CA5) at 4°C overnight. HA matrix was washed with lysis buffer followed by another wash with buffer containing 1 M NaCl, and then eluted with 0.1 M glycine-HCl (pH 2.4) at room temperature for 10 min.

Statistical Analysis

The comparison between two groups was made by t-test (two-tailed), and other comparisons were made by ANOVA followed by Bonferroni's posthoc test. Time-lapse data were assessed by two-way ANOVA repeated measure followed by Bonferroni's posthoc. A value of $p < 0.05$ was considered statistically significant.

Additional methods are found in the supplementary information online.

Acknowledgements

We thank F. Wuytack for SERCA2a and b antibodies. We are grateful for the support to this project from the members of the Suzuki lab. The authors also thank for the technical support from Keiko Shingu and the members of the Takashima Lab on revision. This research was supported by the New Investigator Research Grant from Medical Research Council (G1000461 to Y.S.), Barts and the London Charity and NIHR-Cardiovascular Biomedical Research Unit (to K.S.).

Author contributions: Y.S. conceived and designed research; Y.S., H.C.A.D. and H.K. performed research; Y.S., H.C.A.D., C.M.N.T., S.R.C., H.I., A.W.P., S.T., K.Y. and K.S. analyzed data; H.K., C.M.N.T., S.T., H.I., M.A., J.N., H.S., H.N. and A.W.P. contributed reagents/analytic tools; Y.S. and K.S. wrote the paper.

Conflict of interest

The authors declare that they have no conflict of interest.

References

1. Matzinger P (1994) Tolerance, danger, and the extended family. *Annu Rev Immunol* **12**: 991–1045.
2. Kono H, Rock KL (2008) How dying cells alert the immune system to danger. *Nat Rev Immunol* **8**: 279–289.
3. Haas T, Metzger J, Schmitz F, Heit A, Müller T, Latz E, Wagner H (2008) The DNA sugar backbone 2' deoxyribose determines toll-like receptor 9 activation. *Immunity* **28**: 315–323.
4. Crack PJ, Bray PJ (2007) Toll-like receptors in the brain and their potential roles in neuropathology. *Immunol Cell Biol* **85**: 476–480.
5. Boyd JH, Mathur S, Wang Y, Bateman RM, Walley KR (2006) Toll-like receptor stimulation in cardiomyocytes decreases contractility and initiates an NF-kappaB dependent inflammatory response. *Cardiovasc Res* **72**: 384–393.
6. Shintani Y, Kapoor A, Kaneko M, Smolenski RT, D'Acquisto F, Coppens SR, Harada-Shoji N, Lee HJ, Thiemermann C, Takashima S, et al. (2013) TLR9 mediates cellular protection by modulating energy metabolism in cardiomyocytes and neurons. *Proc Natl Acad Sci USA* **110**: 5109–5114.
7. Brinkmann MM, Spooner E, Hoebe K, Beutler B, Ploegh HL, Kim Y-M (2007) The interaction between the ER membrane protein UNC93B and TLR3, 7, and 9 is crucial for TLR signaling. *J Cell Biol* **177**: 265–275.
8. Kim Y-M, Brinkmann MM, Paquet M-E, Ploegh HL (2008) UNC93B1 delivers nucleotide-sensing toll-like receptors to endolysosomes. *Nature* **452**: 234–238.
9. Kawai T, Akira S (2010) The role of pattern-recognition receptors in innate immunity: update on Toll-like receptors. *Nat Immunol* **11**: 373–384.
10. Zhang L, Rayner S, Katoku-Kikyo N, Romanova L, Kikyo N (2007) Successful co-immunoprecipitation of Oct4 and Nanog using cross-linking. *Biochem Biophys Res Commun* **361**: 611–614.
11. Gingras A-C, Gstaiger M, Raught B, Aebersold R (2007) Analysis of protein complexes using mass spectrometry. *Nat Rev Mol Cell Biol* **8**: 645–654.
12. Palmer AE, Jin C, Reed JC, Tsien RY (2004) Bcl-2-mediated alterations in endoplasmic reticulum Ca²⁺ analyzed with an improved genetically encoded fluorescent sensor. *Proc Natl Acad Sci USA* **101**: 17404–17409.
13. Okada K-I, Minamino T, Tsukamoto Y, Liao Y, Tsukamoto O, Takashima S, Hirata A, Fujita M, Nagamachi Y, Nakatani T, et al. (2004) Prolonged endoplasmic reticulum stress in hypertrophic and failing heart after aortic constriction: possible contribution of endoplasmic reticulum stress to cardiac myocyte apoptosis. *Circulation* **110**: 705–712.
14. Ni L, Zhou C, Duan Q, Lv J, Fu X, Xia Y, Wang DW (2011) β -AR Blockers Suppresses ER Stress in Cardiac Hypertrophy and Heart Failure. *PLoS ONE* **6**: e27294.
15. Glancy B, Balaban RS (2012) Role of Mitochondrial Ca²⁺ in the Regulation of Cellular Energetics. *Biochemistry* **51**: 2959–2973.

16. Rizzuto R, Pozzan T (2006) Microdomains of intracellular Ca²⁺: molecular determinants and functional consequences. *Physiol Rev* **86**: 369–408.
17. Cárdenas C, Miller RA, Smith I, Bui T, Molgó J, Müller M, Vais H, Cheung K-H, Yang J, Parker I, et al. (2010) Essential regulation of cell bioenergetics by constitutive InsP3 receptor Ca²⁺ transfer to mitochondria. *Cell* **142**: 270–283.
18. Kohlhaas M, Maack C (2010) Adverse bioenergetic consequences of Na⁺-Ca²⁺ exchanger-mediated Ca²⁺ influx in cardiac myocytes. *Circulation* **122**: 2273–2280.
19. Iguchi M, Kato M, Nakai J, Takeda T, Matsumoto-Ida M, Kita T, Kimura T, Akao M (2011) Direct monitoring of mitochondrial calcium levels in cultured cardiac myocytes using a novel fluorescent indicator protein, GCaMP2-mt. *Int J Cardiol*.
20. Imamura H, Nhat KPH, Togawa H, Saito K, Iino R, Kato-Yamada Y, Nagai T, Noji H (2009) Visualization of ATP levels inside single living cells with fluorescence resonance energy transfer-based genetically encoded indicators. *Proc Natl Acad Sci USA* **106**: 15651–15656.
21. Kioka H, Kato H, Fujikawa M, Tsukamoto O, Suzuki T, Imamura H, Nakano A, Higo S, Yamazaki S, Matsuzaki T, et al. (2014) Evaluation of intramitochondrial ATP levels identifies G0/G1 switch gene 2 as a positive regulator of oxidative phosphorylation. *Proc Natl Acad Sci USA* **111**: 273–278.
22. Burwell LS, Nadtochiy SM, Brookes PS (2009) Cardioprotection by metabolic shut-down and gradual wake-up. *J Mol Cell Cardiol* **46**: 804–810.
23. Vandecaetsbeek I, Trekels M, De Maeyer M, Ceulemans H, Lescrinier E, Raeymaekers L, Wuytack F, Vangheluwe P (2009) Structural basis for the high Ca²⁺ affinity of the ubiquitous SERCA2b Ca²⁺ pump. *Proc Natl Acad Sci USA* **106**: 18533–18538.
24. Eggermont JA, Wuytack F, Verbist J, Casteels R (1990) Expression of endoplasmic-reticulum Ca²⁺(+)-pump isoforms and of phospholamban in pig smooth-muscle tissues. *Biochem J* **271**: 649–653.
25. Onji M, Kanno A, Saitoh S-I, Fukui R, Motoi Y, Shibata T, Matsumoto F, Lamichhane A, Sato S, Kiyono H, et al. (1AD) An essential role for the N-terminal fragment of Toll-like receptor 9 in DNA sensing. *Nature Communications* **4**: 1949–10.

Figure legends

Figure 1. Identification of SERCA2 as a binding protein of TLR9

(A) Representative image of tandem affinity purification visualized by silverstain is presented. Tandem affinity purification was performed using cardiomyocytes that were adenovirally transfected with TLR9-HA-FLAG or YFP-HA-FLAG. Cardiac fibroblasts transfected with TLR9-HA-FLAG were used as a control. MW: molecular weight markers. Note that the 95-kDa band marked by an asterisk was observed in TLR9 immunoprecipitates from cardiomyocytes, but not from cardiac fibroblasts. (B) CpG-ODN increased the target protein binding to TLR9 (asterisk) in cardiomyocytes.

Figure 2. SERCA2 is a functional adaptor for the alternative TLR9 signalling in cardiomyocytes

(A) Co-immunoprecipitated TLR9 with SERCA2 antibody after cross-linking with DSP was clearly detected in wild-type (WT) mouse neonatal cardiomyocytes. Co-immunoprecipitated TLR9 was abolished in cardiomyocytes from TLR9^{-/-} mice, confirming the specificity of the detecting antibody. Each lane contains proteins immunoprecipitated from 5x10⁶ cells. (B) The overexpressed TLR9 colocalized with SERCA2 at the ER/SR. TLR9-HA-FLAG was expressed in cardiomyocytes and labeled with anti-HA antibody (green) in addition to SERCA2 (red) antibody. (C) Endogenous TLR9 colocalized with SERCA2 in cardiomyocytes. Rat neonatal cardiomyocytes were stained with TLR9 (green) and SERCA2 (red) antibodies at 15 min after CpG-ODN stimulation. The images were obtained by confocal microscope. Scale bar indicates 10 μ m. Experiments were repeated three times and representative images are shown.

Figure 3. TLR9 stimulation decreases SERCA2 activity in cardiomyocytes

(A) RNAi-mediated knockdown of *SERCA2* diminished the TLR9-induced AMPK activation. Different siRNAs targeting SERCA2 similarly inhibited TLR9-induced AMPK activation. Values indicate densitometric ratio of pAMPK/tubulin in immunoblots, mean \pm SEM. The data were obtained from three independent experiments. (B) Ca²⁺-ATPase activity was assessed with microsome fractions from neonatal cardiomyocytes with or without 30 min treatment of CpG-ODN over two different concentrations of free Ca²⁺. The data were obtained from 4 (Ca²⁺; 0.17) or 5 (Ca²⁺; 7.3) preparations in each group. (C) FRET/CFP emission ratio plots of SR/ER Ca²⁺ probe in cardiomyocytes treated with control ($n=26$) or CpG-ODN ($n=27$). CpG-ODN significantly reduced SR/ER Ca²⁺ in neonatal cardiomyocytes after CpG-ODN. The measurements were normalized to the ratio at time 0. (D) Representative FRET/CFP ratiometric pseudocolored images of SR/ER Ca²⁺ probe in cardiomyocytes treated with control or CpG-ODN. Scale bar indicates 10 μ m. (E) Ca²⁺ content, as assessed by the amplitude of the caffeine-induced Fluo-4 transient in adult rat cardiomyocytes, was significantly decreased after CpG treatment ($n=28$) compared to the control ($n=26$). (F) Representative traces of cytosolic Fluo-4 transients from the control (black; $n=50$) and CpG-ODN (red; $n=51$) treated cardiomyocytes elicited at 0.5 Hz pacing. (G) Time to peak and time to 50% decay of the Fluo-4

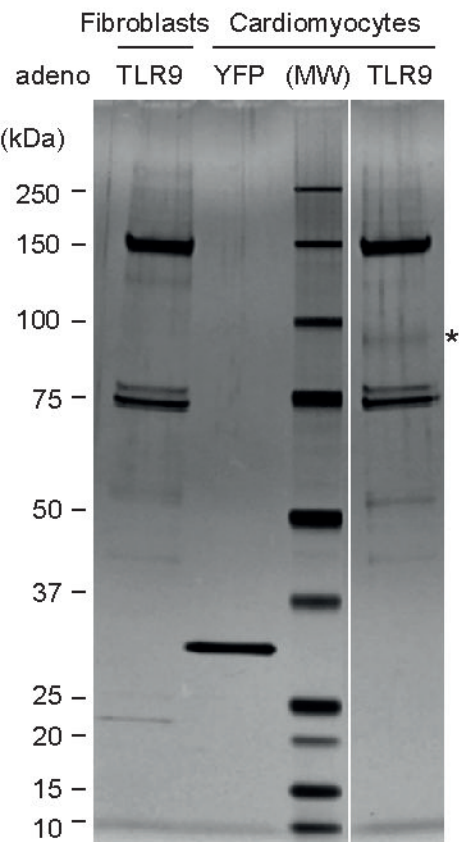
transients were both delayed by CpG stimulation. Also, the amplitude of the Fluo-4 transients (F/F_0) was decreased by CpG stimulation. (H) Thapsigargin (500 ng/ml for 0, 15, 30 min) increased pAMPK without administration of CpG-ODN. The data were obtained from three independent experiments. (I) CpG-ODN administration did not induce ER stress that was assessed by the expression level of *GRP78* and *94* that was measured by realtime PCR in rat cardiomyocytes treated with CpG-ODN for the indicated period. * $p < 0.05$ ** $p < 0.01$ *** $p < 0.001$ compared with the control. Error bars indicate SEM.

Figure 4. TLR9 decreases the mitochondrial ATP synthesis by altering $[Ca^{2+}]_m$ via SERCA2

(A, B) Time-lapse analysis of mitochondrial matrix Ca^{2+} in G-CaMP2-mt transfected cardiomyocytes after the vehicle control ($n=25$; circle) or CpG-ODN ($n=20$; triangle) administration. CpG administration significantly reduced mitochondrial Ca^{2+} in cardiomyocytes. Representative images with pseudocolor for each condition are shown in (A). (C) Adenovirus-mediated transfection of mit-ATeam showed mitochondrial localization in rat cardiomyocytes, which enabled to monitor the mitochondrial ATP levels. (D) Time-lapse analysis of mitochondrial ATP levels in mit-ATeam transfected cardiomyocytes after the vehicle control ($n=13$; circle), CpG-ODN ($n=11$; triangle) or Oligomycin ($n=11$; square), an inhibitor of ATP synthase used as a positive control. Mitochondrial ATP levels significantly dropped after CpG stimulation in cardiomyocytes. Scale bars indicate 10 μm . Error bars indicate SEM. ** $p < 0.01$ *** $p < 0.001$ compared with the control. (E) Schematic presentation of two different TLR9 signalling pathways. Cardiomyocytes or neurons sense DNA (danger signal) upon tissue injury, reduce energy metabolism by alteration of microdomain Ca^{2+} handling through SERCA2, and consequently increase the stress tolerance through AMPK activation, while immune cells initiate the inflammatory response.

Figure 1

A



B

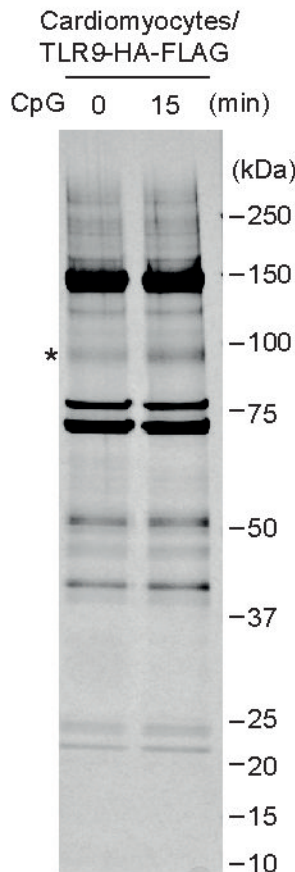
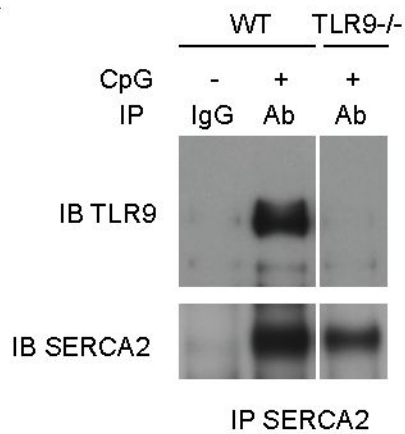
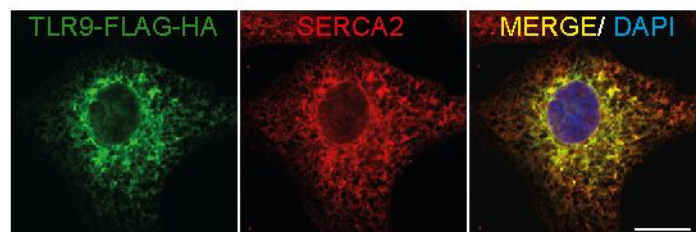


Figure 2

A



B



C



Figure 3

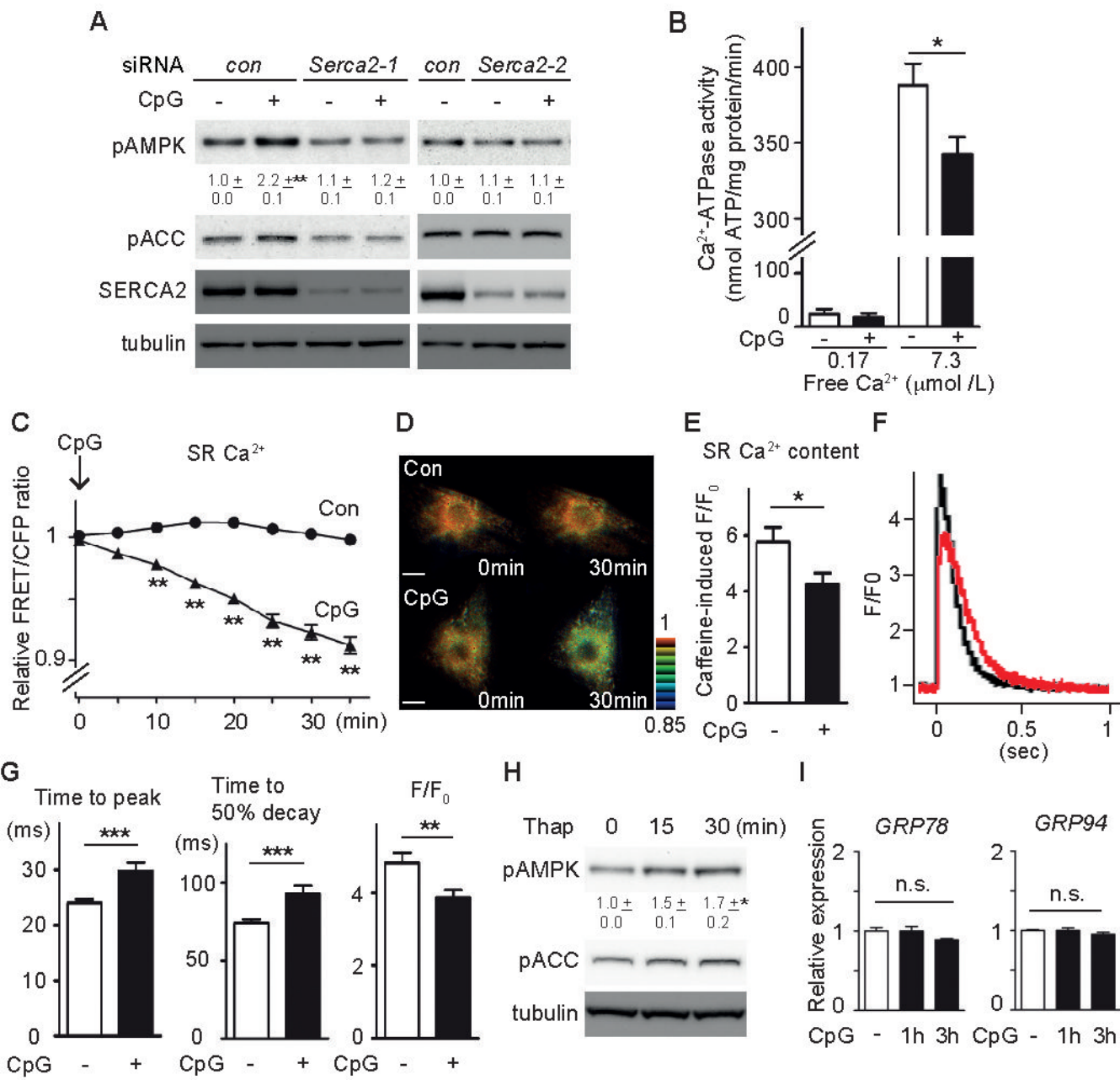
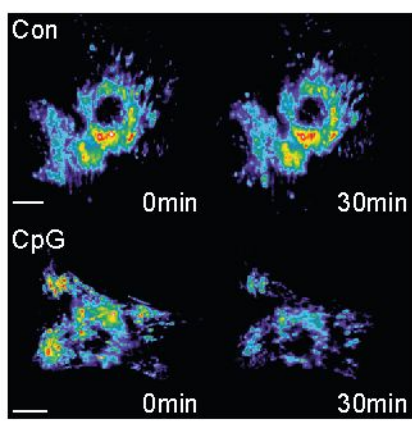
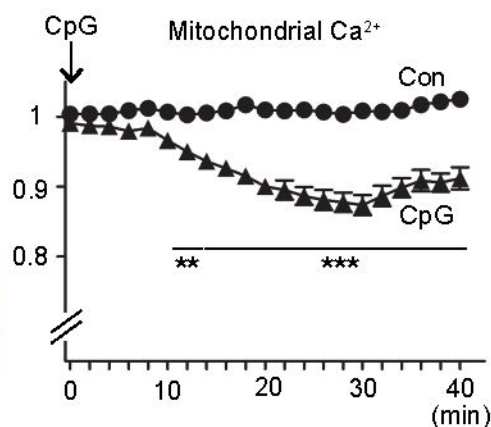


Figure 4

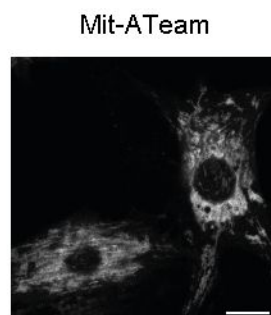
A



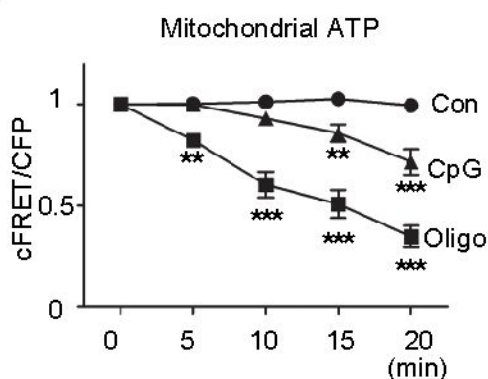
B



C



D



E

